



The role of Eu_2O_3 and CeO_2 on the phase formation, infrared emission and magnetic properties of $\text{Co}_{0.6}\text{Zn}_{0.4}\text{Fe}_2\text{O}_4$ ceramics by a solvothermal method

Ying Zhang, Ji Ma, Juan Lu*, Dijiang Wen

Inorganic Materials Department, College of Chemistry, Chemical Engineering and Materials Science, Soochow University, Suzhou 215123, China

Received 12 July 2013; received in revised form 17 August 2013; accepted 27 August 2013

Available online 8 September 2013

Abstract

Nanosized Eu_2O_3 and CeO_2 co-addition CoZn ceramics have been achieved via a hydrothermal method by adjusting the mol ratios of Eu and Ce. The as-prepared samples were characterized by X-ray diffraction (XRD), Transmission electron microscopy (TEM), Fourier transform infrared (FTIR), Vibrating sample magnetometer (VSM) and Infrared emission measurement (IRE-2). The particle morphologies of the as-prepared samples evolve from spherical, to self-assembled nanoparticles, and irregular nanoparticles when the mol ratios (x) of Eu and Ce was changed from 0:10 to 10:0. Correspondingly, the main phases of the as-prepared samples change from both cubic spinel CoFe_2O_4 and CeO_2 , pure cubic cerianite CeO_2 , to amorphous. Meanwhile, the as-prepared samples appear transformed from a ferromagnetic behavior with a saturation magnetization 66.4 emu/g to a paramagnetic behavior with a saturation magnetization of 0.55 emu/g at turning point $x=3.5:6.5$. While the infrared emissivity is increasing as the x from 0:10 to 3.5:6.5, reach the maximum at 3.6:6.4, and then remain stable when further increasing x till 10:0. Those may be due to the amorphous tendency rising and the particle sizes gradual decreasing with x increasing from 0:10 to 10:0. What is more important is that the solvothermal method is proved to be an efficient way to prepare CoZn nano-ceramics in this study which may open new pathways to magnetic and far infrared therapy.

© 2013 Elsevier Ltd and Techna Group S.r.l. All rights reserved.

Keywords: Infrared emission property; Magnetic property; Hydrothermal method; CoZn ceramics

1. Introduction

$\text{Co}_{0.6}\text{Zn}_{0.4}\text{Fe}_2\text{O}_4$ (CoZn) ferrite ceramic is a kind of spinel-structured material with good magnetic and infrared emission properties, which can be widely used in many fields, such as magnetic therapy and far infrared therapy. The key to promote its applications in those areas is not only having stable magnetism and high infrared emissivity, but also having small particle size (such as nanoscale). The microstructure and physical properties of ceramics are highly sensitive to composition, grain size, the nature and amount of any additives and impurities and the preparation method [1–3]. Therefore, the doping modification and processing methods are critical

factors that determine the magnetic and far infrared emission properties of CoZn ceramic.

Meanwhile, CoZn ferrite ceramic is polycrystals, which tends to have the mixed spinel structure. The octahedral coordinated high spin Fe^{3+} ions exhibit a strong spin–orbital coupling. If the partial substitution of RE^{3+} —the 4f elements series—for Fe^{3+} ones in CoZn ferrite ceramic will be promising to manipulate magnetic coupling and lattice vibration [4,5]. This is contributive to the magnetic and infrared emission property. In our previous studies, the co-doping of RE (La, Ce, Pr, Nd, Sm, Eu, Gd, Tb and Dy) and Mn ions has been significantly improved the magnetic and infrared emission properties of CoZn ferrite ceramics synthesized by the solid-state reaction method [1,6]. The main reason is the synergistic effect caused by co-doping that is beneficial to the improvement of magnetic and infrared emission properties of the CoZn ferrite ceramic. Therefore, given the large diversity in lanthanide oxides, we selected a couple of

*Corresponding author. Tel./fax: +86 512 65880089.

E-mail address: lujuan@suda.edu.cn (J. Lu).

representative oxides—Ce and Eu oxides—to study their conjugate effect in terms of co-addition for CoZn ceramics. While the conjugate effect of Ce and Eu ions has been confirmed in the luminescent properties of ceramics [7,8]. As the Ce and Eu ions have a similar radius, which is larger than that of Fe^{3+} ions, adding Ce and Eu into the crystal structure of CoZn ceramic might introduce lattice distortion and cation disorder that may manipulate magnetic coupling and lattice asymmetrical vibrations. Therefore, selecting co-addition of CeO_2 and Eu_2O_3 may be an efficient way to improve the magnetic and infrared emission properties of CoZn nano-ferrite.

Although the CoZn ceramics prepared by solid-state reaction method has good magnetic properties and infrared emission properties in the 8–14 μm spectral wavelength ranges at room temperature, it also has high coercivity and large grain size (microscale) [1,6]. This is bad for application in magnetic therapy and far infrared therapy. Therefore, it is urgent to find a new prepared method to obtain a kind of material, which has the low coercivity and nanoscale particle size. So far, many methods for synthesizing CoZn ceramic have been reported, including the ceramic method [9,10], the Chimie douce route [4], the co-precipitation [11], forced hydrolysis [12], the sol-gel method [13], the combustion method [14] and the solvothermal method [15]. Among them, the solvothermal method seems to be one of the effective methods, because it is quite simple, easily obtains the high crystallinity of the nano-materials at a relatively low temperature ($T \sim 200^\circ\text{C}$), has the capability to control crystal growth and prepares large quantities of nano-ceramics.

Besides that, the distribution of Eu and Ce ions in the CoZn structure will be different prepared by solid-state reaction method or solvothermal method, especially when they were introduced in the form of oxides. This will in turn influence the microstructure and properties of CoZn nano-ceramics. Therefore, the aim of the present study is to follow the evolution of structure of Eu and Ce co-addition CoZn ceramics prepared by a solvothermal method, and to connect it with their magnetic and infrared emission properties.

2. Experimental

2.1. Synthesis of CoZn nanoceramics

Precursors, comprising hydrated iron (III) nitrate, hydrated zinc nitrate, hydrated cobalt (II) nitrate, Ce_2O_3 and Eu_2O_3 were dissolved in 50 ml of ethylene glycol according the desired proportions $\text{Co}_{0.6}\text{Zn}_{0.4}(\text{Eu}, \text{Ce})_{0.1}\text{Fe}_{1.9}\text{O}_4$ to prepare Eu_2O_3 and CeO_2 co-addition CoZn nano-ceramics. Among them, the Eu/Ce mol ratio is denoted with x ($x=0:10, 2:8, 3.5:6.5, 3.6:6.4, 4:6, 6:4$ and $10:0$), while the $\text{Co}_{0.6}\text{Zn}_{0.4}\text{Fe}_2\text{O}_4$ ferrite ceramic is named as UF. Then, 0.02 mol of anhydrous sodium acetate and 1 ml of polyethylene glycol were added into the solution under vigorous stirring at room temperature for 0.5 h. Subsequently, the mixture was added into a 100 ml Teflon-sealed autoclave and maintained at 200°C for 12 h. Then, the mixture was cooled to room temperature. The product was collected with a magnet, cleaned by four cycles of washing/

redispersion in anhydrous ethanol and dried in vacuum at 80°C for 12 h.

2.2. Characterization

The microstructure of samples were tested by a X-ray diffractometer (XRD, Model D/MAX-III, Japan) ($\text{Cu K}\alpha$) with a step size of 0.02° and 2θ range from 20° to 80° . The morphology and particle sizes were taken using transmission electrical microscopy (TEM, TecnaiG220, America). Infrared spectra of composites were recorded on the infrared spectrometer (FTIR, Model Nicolet 5700, USA), measured as a KBr pellet in the $400\text{--}4000\text{ cm}^{-1}$ spectral range. Infrared emission properties were examined using an infrared emission tester (Model IRE-2, China) at room temperature. Magnetic measurements were carried out at room temperature using a vibrating sample magnetometer (VSM, Model BHV-55, Japan) with a maximum magnetic field of 20,000 Oe.

3. Results and discussion

3.1. XRD analysis

The XRD patterns of the as-prepared samples under investigation, shown in Fig. 1, indicate that the phase composition of samples has greatly changed with the mol ratios of Eu and Ce. All peaks of the sample UF are characteristics for the cubic structure and spinel-type lattice of CoFe_2O_4 (JCPDS 22-1086) without any second phases detected. The sharp diffraction peaks indicate the good crystallinity of the nano-ceramics. The lattice parameter estimated from the strongest diffraction peak of (311) is 8.379 \AA , which is consistent with the bulk value (8.377 \AA) of CoFe_2O_4 . In the case of Eu_2O_3 and CeO_2 co-addition samples, below $x=3.5:6.5$, the CoFe_2O_4 spinel phase accompanied with crystalline CeO_2 phase (JCPDS 04-0593) are observed. Moreover, the intensities of diffraction peaks significantly reduce and the widths of diffraction peaks accordingly broaden with x further increasing, indicating the poor crystallinity and ultra-fine nature of the particles. The most likely explanation for this is that the added CeO_2 and Eu_2O_3 , during the solvothermal synthesis process, will diffuse into the grain boundaries and form an isolating ultra-thin layer around the grains, which is possible to restrain the formation of CoFe_2O_4 spinel phase [16]. In addition, with further increasing the mol ratios of Eu and Ce, the samples only exhibit a single CeO_2 phase without CoFe_2O_4 spinel phase (above $x=3.6:6.4$). Finally, when x equals to $10:0$, the as-prepared sample is nearly amorphous-like (weak crystalline) characterized by the diffuse humps. Meanwhile, no extra reflections corresponding to the oxides of Eu can be found, and only significant reduction of the strongest peaks is obtained with increasing the values of x . Therefore, we consider that the rare earth ions cannot form solid solution in the CoZn ceramics under this synthesis condition. However, the CeO_2 and Eu_2O_3 co-addition behavior still has an important influence on the phase composition and structure of CoZn nano-ceramics.

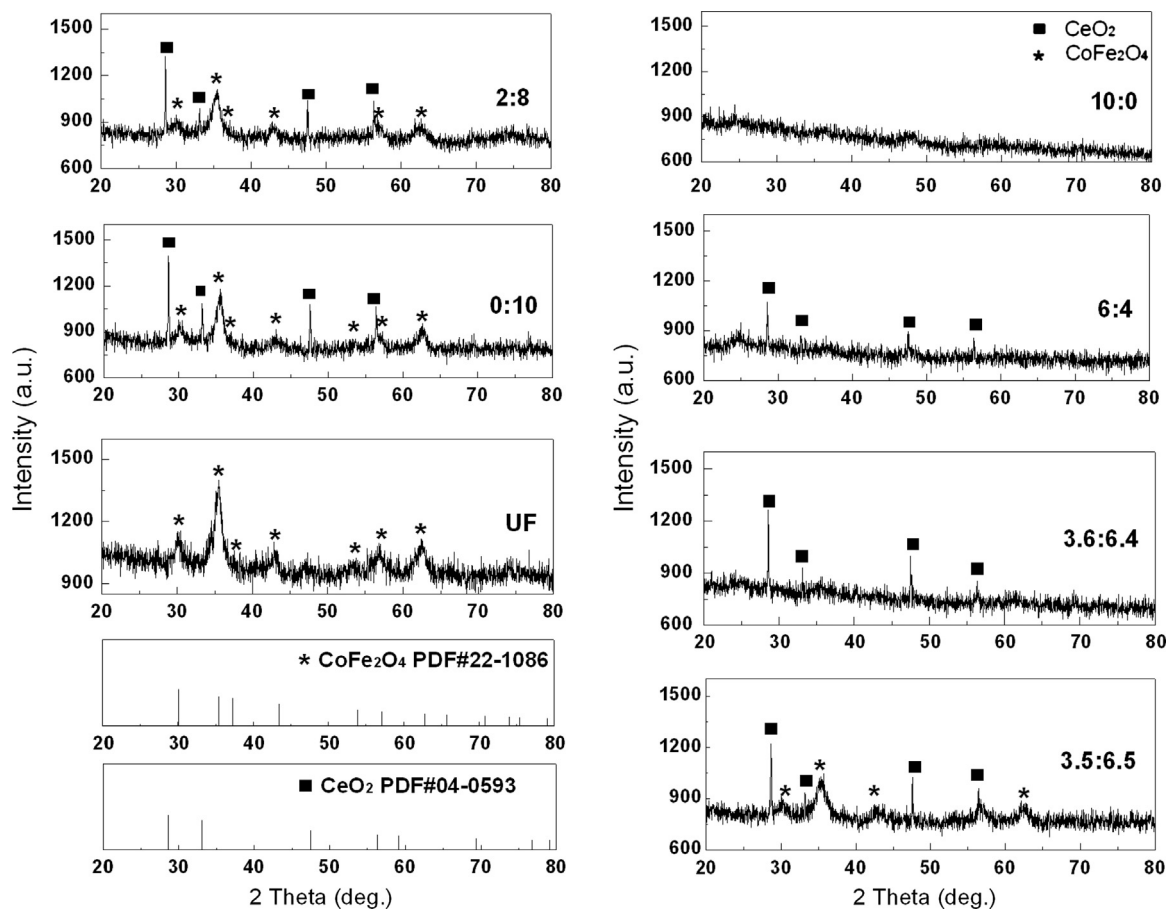


Fig. 1. XRD patterns of $\text{Co}_{0.6}\text{Zn}_{0.4}\text{Fe}_2\text{O}_4$ (UF), and Eu_2O_3 and CeO_2 co-addition $\text{Co}_{0.6}\text{Zn}_{0.4}\text{Fe}_2\text{O}_4$ nano-ceramics, among them, the Eu/Ce mol ratio is 0:10, 2:8, 3.5:6.5, 3.6:6.4, 6:4 and 10:0.

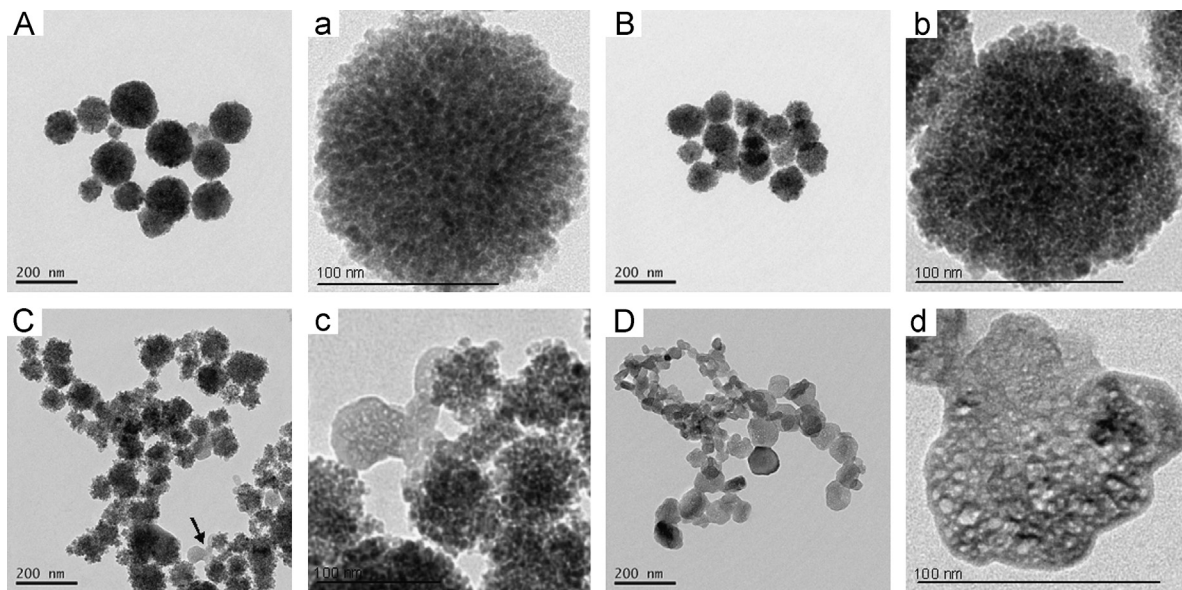


Fig. 2. Typical TEM images of $\text{Co}_{0.6}\text{Zn}_{0.4}\text{Fe}_2\text{O}_4$ (A), and Eu_2O_3 and CeO_2 co-addition $\text{Co}_{0.6}\text{Zn}_{0.4}\text{Fe}_2\text{O}_4$ nano-ceramics, among them, the Eu/Ce mol ratio is 0:10 (B), 3.5:6.5 (C) and 10:0 (D); a–d are the higher magnification TEM images of samples accordingly.

3.2. TEM analysis

The morphology and size of the self-assembly CoZn magnetic nano-particles are characterized by TEM. The representative TEM

micrographs of the typical samples are shown in Fig. 2. The graphs reveal that the sample UF is spherical particle with an average diameter of 100–200 nm, which is constructed with many tiny nanocrystallites with an average size of 5–10 nm (Fig. 2(A))

and (a)). The average particle sizes of the CeO_2 and Eu_2O_3 co-addition samples have obviously decreased compared with that of the sample UF (Fig. 2(b)–(d)), in contrast to the results reported for similar materials prepared by a ceramic route [17]. Another interesting phenomenon is the formation of amorphous-like phase in Fig. 2, especially in Fig. 2(C), which means that with increasing the values of x , the as-prepared samples tend to become amorphous state. As we known, during the hydrothermal process, the competition between crystal nucleation and crystal growth determines the size of the products [18]. The crystal size will be small on condition that the rate of crystal nucleation is greater than that of crystal growth. Therefore, in our experiment, Eu and Ce ions evidently played a key role in limiting the growth speed of spinel crystals. However, with x increasing, the surface of CoZn ceramics tend to amorphous state and become clearly with x to 10:0. This is in agreement with XRD patterns above. According to the literature, different factors may affect nanoparticles morphology. Therefore, in the present case, changes in CoZn ceramics morphology are to be attributed to the changes in mol ratios of Eu and Ce, probably promoting the polycrystal structure transformed to amorphous structure.

3.3. Infrared analysis

Fig. 3 shows the FTIR spectra of CoZn nano-ceramics. The adsorbed water is featured by bands around $3410\text{--}3430\text{ cm}^{-1}$ and $1640\text{--}1660\text{ cm}^{-1}$ which can be observed in all of the CoZn nano-ceramics, assigned to O–H stretching and H–O–H bending modes of vibration respectively. The two prominent absorption bands ν_1 and ν_2 respectively existing at around 600 and 400 cm^{-1} in

samples CoZn nano-ceramics ($x \leq 3.5:6.5$) correspond to the tetrahedral complexes and octahedral complexes [19,20], implying the formation of the spinel ferrite phase (Fig. 3(a)). It shows that both the positions of ν_1 and ν_2 bands are almost constant in Fig. 3 (a) which indicates that the cation distribution in the octahedral and tetrahedral sites seems almost uninfluenced in Eu_2O_3 and CeO_2 co-addition CoZn ceramics. In addition, with increasing the values of x , the intensities of those bands decrease, and even become less pronounced (Fig. 3(b)), which also confirms the disappearance of octahedral and tetrahedral vibration. The FTIR analyses agree well with XRD results.

It is interesting to compare the FTIR spectra of sample $x=3.5:6.5$ with that of sample $x=3.6:6.4$. For the sample $x=3.5:6.5$, the FTIR spectrum exhibits two obvious frequency absorption bands at 419 cm^{-1} and 588 cm^{-1} (Fig. 4). These bands may be associated with the presence of spinel CoFe_2O_4 . For the sample $x=3.6:6.4$, the vibrational behavior was apparently modified and three high-frequency adsorption bands at 490 cm^{-1} , 540 cm^{-1} and 630 cm^{-1} are detected after only a single CeO_2 phase exists. This also indicates the disappearance of octahedral and tetrahedral vibration belonging to CoFe_2O_4 in the samples, above $x=3.5:6.5$.

3.4. Infrared emission properties analysis

Far infrared emissivity is of great importance to determine the infrared emission properties of materials, particularly in the $8\text{--}14\text{ }\mu\text{m}$ spectral wavelength range, and the far infrared emission properties of spinel ceramic relate to the lattice asymmetrical vibration within this range. The lower the lattice

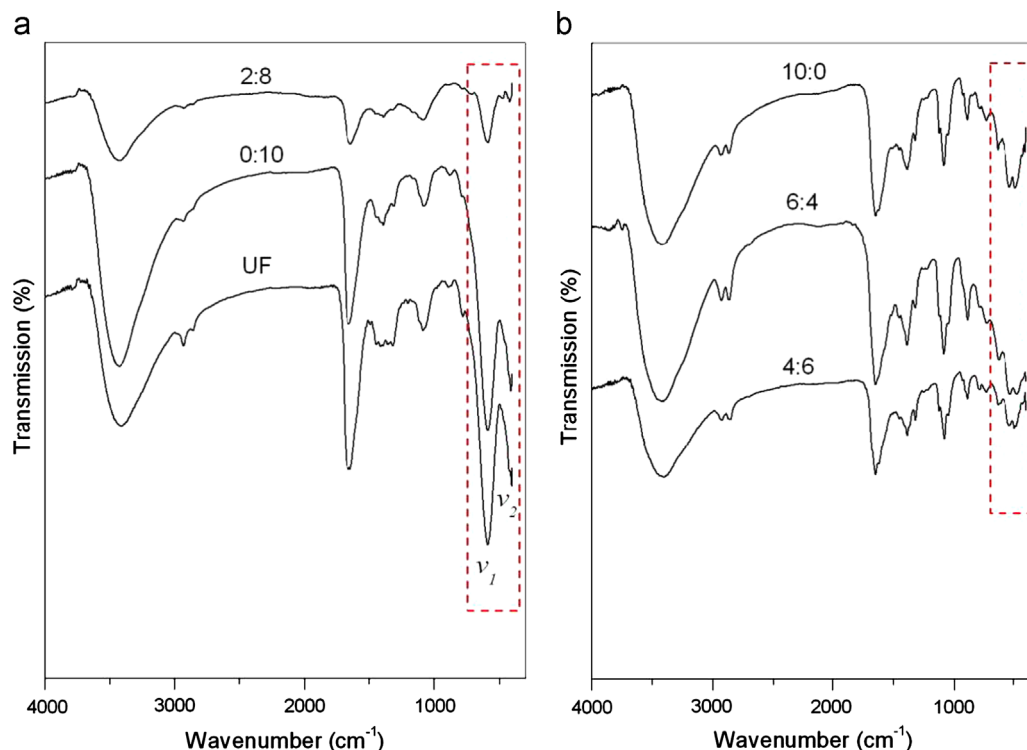


Fig. 3. FTIR spectra of samples. (a) $\text{Co}_{0.6}\text{Zn}_{0.4}\text{Fe}_2\text{O}_4$ (UF), and Eu_2O_3 and CeO_2 co-addition $\text{Co}_{0.6}\text{Zn}_{0.4}\text{Fe}_2\text{O}_4$ nano-ceramics, among them, the Eu/Ce mol ratio is 0:10 and 2:8. (b) Eu_2O_3 and CeO_2 co-addition $\text{Co}_{0.6}\text{Zn}_{0.4}\text{Fe}_2\text{O}_4$ nano-ceramics, among them, the Eu/Ce mol ratio is 4:6, 6:4 and 10:0.

vibration symmetry is, the greater the dipole matrix change is and the higher the far infrared emissivity is.

Experiments prove that far infrared emissivity could be effectively enhanced by additives. The mechanisms for additive enhancing emissivity in the wavelength range of 8–14 μm were proposed, such as cations redistribution in tetrahedral and

octahedral sites [21], distortion of the crystal lattice [22], etc. The variation of infrared emissivity of the CoZn nano-ceramics as function of the mol ratios of Eu and Ce is shown in Fig. 5(a). It can be observed that the values of far infrared emissivity are increasing with x from 0:10 to 3.5:6.5, reach the maximum at 3.6:6.4, and then remain stable when further increasing x till 10:0. The variation of far infrared emissivity as a function of x is obvious, which agrees with the results of XRD and FTIR analyses, suggesting that the rare earth ions would like to gather on the grain boundaries or on the surface rather than to form solid solution in the spinel ceramics under this synthesis condition. The grain size of as-prepared samples is smaller than the wavelength of the infrared emission, which reduced the scattering coefficient and enhances the infrared emission of CoZn nano-ceramics within the 8–14 μm spectral wavelength ranges. Therefore, the changing of far infrared emissivity is not all regard of cation redistribution in the tetrahedral and octahedral sites but of the grain size in our experiment. The results indicate the solvothermal prepared CoZn nano-ceramics have the better infrared emission properties for their small grain size, high specific surface area and activity, causing distortion of the crystal lattice and shrinkage of the unit cell volume. This in turn decreases the symmetry of the lattice vibration, and enhances the effects of a harmonic vibration of polar lattice, the coupled action of phonon, and phonon combination emission, and thus the far infrared emissivity is strengthened [23,24].

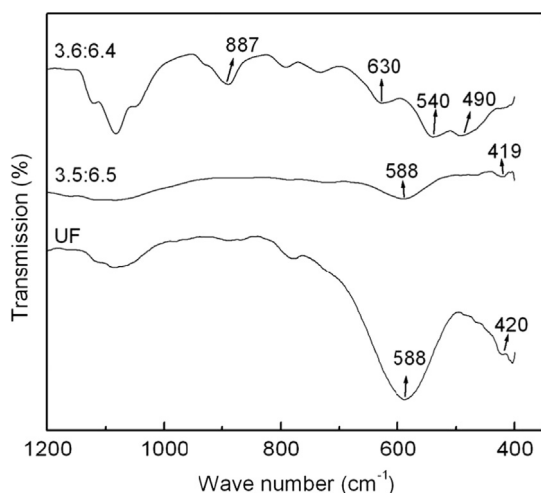


Fig. 4. Typical FTIR spectra in the 1200–400 cm^{-1} region of $\text{Co}_{0.6}\text{Zn}_{0.4}\text{Fe}_2\text{O}_4$ (UF), and Eu_2O_3 and CeO_2 co-addition $\text{Co}_{0.6}\text{Zn}_{0.4}\text{Fe}_2\text{O}_4$ nano-ceramics, among them, the Eu/Ce mol ratio is 3.5:6.5 and 3.6:6.4.

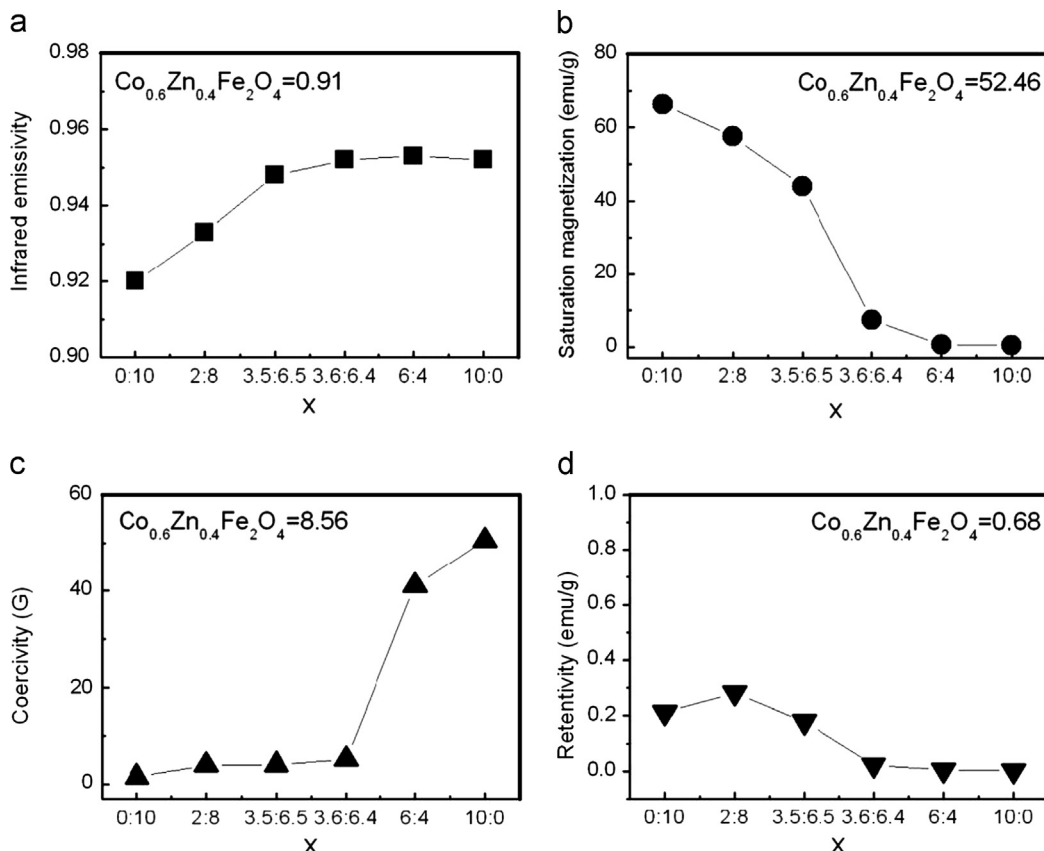


Fig. 5. Variation of far infrared emissivity and magnetic parameters of Eu_2O_3 and CeO_2 co-addition $\text{Co}_{0.6}\text{Zn}_{0.4}\text{Fe}_2\text{O}_4$ nano-ceramics, among them, the Eu/Ce mol ratio is 0:10, 2:8, 3.5:6.5, 3.6:6.4, 6:4 and 10:0, (a) far infrared emissivity; (b) saturation magnetization; (c) coercivity and (d) retentivity.

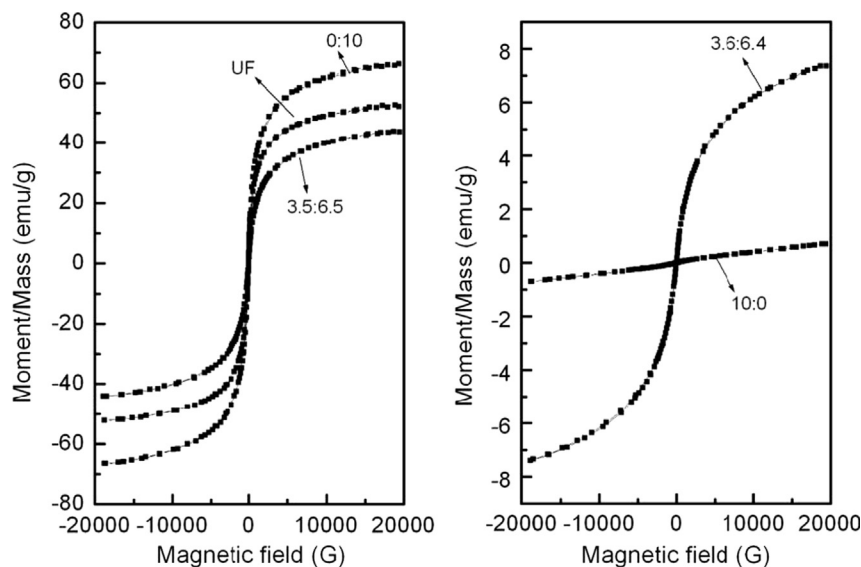


Fig. 6. Typical magnetic hysteresis loops of $\text{Co}_{0.6}\text{Zn}_{0.4}\text{Fe}_2\text{O}_4$ (UF), and Eu_2O_3 and CeO_2 co-addition $\text{Co}_{0.6}\text{Zn}_{0.4}\text{Fe}_2\text{O}_4$ nano-ceramics, among them, the Eu/Ce mol ratio is 0:10, 3.5:6.5, 3.6:6.4, and 10:0.

3.5. Magnetic properties analysis

Fig. 6 shows the change in the hysteresis loops of the sample CoZn nano-ceramics as a function of x at room temperature. It could be observed that the sample ($0:10 \leq x \leq 3.5:6.5$) shows a typical paramagnetic behavior as the coercivity is almost negligible, while the sample ($3.5:6.5 < x \leq 10:0$) shows a ferromagnetic behavior. The saturation magnetization values are greatly affected by increasing the values of x because of the gradual increase in the crystallinity and particle size. The maximum saturation magnetization of 66.4 emu/g obtained for sample $x=0:10$, followed by 57.6 emu/g for sample $x=2:8$, which is higher than that of sample UF (52.5 emu/g). This illustrates the Eu_2O_3 and CeO_2 co-addition could help to improve the magnetic properties of CoZn nano-ceramics. Meanwhile, the coercivity increases with increasing the values of x , while the retentivity is almost negligible.

The reason for this can be considered to be its complex crystalline structure. Co-addition of Eu_2O_3 and CeO_2 resulted in various phases such as CoFe_2O_4 , CeO_2 or mixed phases between CoFe_2O_4 and CeO_2 and brought about the decrease in crystallinity and grain size all together. The changes in the magnetic parameters with the values of x are shown in Fig. 5(b)–(d). Therefore, the local structure effect must be considered in order to understand the magnetic properties evolution in the CoZn nano-ceramics.

The general formula of the spinel ceramic is AB_2O_4 in that the cations reside on tetrahedral and octahedral sites. In this cubic structure, only one eighth of tetrahedral and half of octahedral sites are occupied by cations. The variation of cation distribution over the tetrahedral and octahedral sites in the spinel ceramic would lead to different magnetic properties [25]. The CoZn ceramics are mixed spinel structure determined by the site occupancy of cation in the tetrahedral and octahedral sites, forming ZnFe_2O_4 and CoFe_2O_4 spinel phases. ZnFe_2O_4 phase is a normal phase, where all Zn^{2+} ions preferably occupy the tetrahedral sites, exhibiting lower magnetic moment at room temperature [26]. While CoFe_2O_4

phase is typically an inverse ferrite with all Co^{2+} ions located in the octahedral sites, possessing higher magnetization (~ 80 emu/g) at room temperature [27]. In the ideal situation, where the ferrite phases adopt a pure inverse-type spinel structure (CoFe_2O_4), the magnetization per formula unit is represented by the net moment of that in tetrahedral and octahedral sites.

From the results of XRD and FTIR, it can be found the two phases of CoFe_2O_4 and CeO_2 coexist in the CoZn nano-ceramics when the values of x is between 0:10 and 3.5:6.5. The CoZn nano-ceramics show the paramagnetic behavior with the saturation magnetization from 66.4 to 44.0 emu/g at the moment. When the values of x are above 3.5:6.5, the value of saturation magnetization is close to zero, and only a single CeO_2 phase exists. The most obvious example is the sample $x=10:0$ whose saturation magnetization value is 0.55, tending to zero, because of the amorphous. Both the structure's turning point (Figs. 1 and 3) and the magnetic property's turning point (Fig. 5) occur in the sample $x=3.5:6.5$. The experiments results show that the change of main phase causes the change of crystal structure and further causes the change of magnetic properties in the CoZn nano-ceramics. In turn, the CoZn ceramics go from being paramagnetic behavior to ferromagnetic behavior with x increasing.

4. Conclusions

Using solvothermal method, Eu_2O_3 and CeO_2 co-addition CoZn nano-ceramics have been synthesized. The role of Eu_2O_3 and CeO_2 co-addition on the phase formation, morphology, magnetic and far infrared emission properties of the CoZn ceramics have been studied in detail. From the results obtained, it is obvious that the co-addition of Eu_2O_3 and CeO_2 plays vital roles in microstructures, which subsequently results in the tuning magnetic and far infrared emission properties of CoZn nano-ceramics. The nano-ceramics with doping mol ratios $0:10 \leq x \leq 3.5:6.5$ were CoFe_2O_4 spinel phase accompanied with crystalline CeO_2 phase, which shows a typical paramagnetic behavior, the

coercivity is almost negligible and the far infrared emissivity increases at this time. While the doping mol ratios $3.5:6.5 < x \leq 10:0$ were only crystalline CeO_2 phase that shows a ferromagnetic behavior, the far infrared emissivity tend to constant.

The difference between the samples might be due to two reasons: Firstly, the distortion in grain boundaries that caused by finer grain size can hamper the process of magnetization. Secondly, the complex crystalline phase caused by Eu_2O_3 and CeO_2 co-addition can change the magnetization. Therefore, the effective magnetic field might be smaller than actual magnetic field. All of these might make it difficult to magnetize the Eu_2O_3 and CeO_2 co-addition CoZn nano-ceramics. In summary, the special structure of the CoZn nano-ceramics caused by Eu_2O_3 and CeO_2 co-addition has a significant impact on the magnetic and infrared emission properties. Such a combination of Eu_2O_3 and CeO_2 in the CoZn ceramic should create novel magnetic and infrared emission properties and relevant ideas could inspire the investigation of multifunctional materials. Further researches are needed to get a better performance by combination with dyeing of silk fabric.

It can be seen the change of magnetic and infrared emission properties is interesting but very complicated, the major effects being observed for the synergistic effect caused by Eu_2O_3 and CeO_2 co-addition. Anyhow, that hydrothermal is a simple and fast method even for large amount of CoFe_2O_4 nanocrystals, and the solvothermal prepared samples—a nano-material both with the magnetic and infrared emission properties—can be used as the magnetic therapy and far infrared therapy media.

Acknowledgments

This research was supported by the Universities Natural Science Research Project of Jiangsu Province (11KJD430004) and the Priority Academic Program Development of Jiangsu Higher Education Institution (PAPD).

References

- [1] Y. Zhang, D.J. Wen, Infrared emission properties of RE (RE=La, Ce, Pr, Nd, Sm, Eu, Gd, Tb, and Dy) and Mn co-doped $\text{Co}_{0.6}\text{Zn}_{0.4}\text{Fe}_2\text{O}_4$ ferrites, *Materials Chemistry and Physics* 131 (2012) 575–580.
- [2] D. Varshney, K. Verma, A. Kumar, Substitutional effect on structural and magnetic properties of $\text{A}_x\text{Co}_{1-x}\text{Fe}_2\text{O}_4$ (A=Zn, Mg and $x=0.0, 0.5$) ferrites, *Journal of Molecular Structure* 1006 (2011) 447–452.
- [3] M. Mozaffari, S. Manouchehri, M.H. Yousefi, The effect of solution temperature on crystallite size and magnetic properties of Zn substituted Co ferrite nanoparticles, *Journal of Magnetism and Magnetic Materials* 322 (2010) 383–388.
- [4] L.B. Tahar, M. Artus, S. Ammarb, L.S. Smiri, F. Herbst, M.J. Vaulay, V. Richard, J.M. Grenèche, F. Villain, F. Fiévet, Magnetic properties of $\text{CoFe}_{1.9}\text{RE}_{0.1}\text{O}_4$ nanoparticles (RE=La, Ce, Nd, Sm, Eu, Gd, Tb and Ho) prepared in polyol, *Journal of Magnetism and Magnetic Materials* 320 (2008) 3242–3250.
- [5] J.C.G. Bünzli, G.R. Choppin, *Lanthanide Probes in Life, Chemical and Earth Sciences, Theory and Practice*, Elsevier, Amsterdam, 1989.
- [6] Y. Zhang, D.J. Wen, The effect of cation distribution on magnetic and infrared emission properties of RE^{3+} , MnO_2 : CoZn (RE=La, Ce, Pr, Nd, Sm, Eu, Gd, Tb and Dy) ferrite ceramics, *Journal of the American Ceramic Society* 95 (2012) 2919–2927.
- [7] K.W. Chae, T.R. Park, C. Cheon, N.I. Cho, J.S. Kim, Enhanced phase miscibility and luminescence by inducing oxygen vacancies in $\text{Ce}_{1-x}\text{Eu}_x\text{O}_{2-\delta}$ under a strongly reducing atmosphere, *Journal of Luminescence* 136 (2013) 109–116.
- [8] V.B. Pawade, S.J. Dhoble, Blue emission in Eu^{2+} and Ce^{3+} activated novel aluminates based phosphors, *Journal of Luminescence* 135 (2013) 318–322.
- [9] A. Tawfik, Electromechanical properties of $\text{Co}_{0.6}\text{Zn}_{0.4}\text{Fe}_2\text{O}_4$ ferrite transducer, *Journal of Magnetism and Magnetic Materials* 237 (2001) 283–287.
- [10] A. Tawfik, I.M. Hamada, O.M. Hemeda, Effect of laser irradiation on the structure and electromechanical properties of Co–Zn ferrite, *Journal of Magnetism and Magnetic Materials* 250 (2002) 77–82.
- [11] R. Arulmurugana, G. Vaidyanathana, S. Sendhilnathanb, B. Jeyadevan, Thermomagnetic properties of $\text{Co}_{1-x}\text{Zn}_x\text{Fe}_2\text{O}_4$ ($x=0.1-0.5$) nanoparticles, *Journal of Magnetism and Magnetic Materials* 303 (2006) 131–137.
- [12] S.T. Alone, S.E. Shirsath, R.H. Kadam, K.M. Jadhav, Chemical synthesis, structural and magnetic properties of nano-structured Co–Zn–Fe–Cr ferrite, *Journal of Alloys and Compounds* 509 (2011) 5055–5060.
- [13] L.Z. Li, L. Peng, Y.X. Li, X.H. Zhu, Structure and magnetic properties of co-substituted NiZn ferrite thin films synthesized by the sol–gel process, *Journal of Magnetism and Magnetic Materials* 324 (2012) 60–62.
- [14] M.H. Yousefi, S. Manouchehri, A. Arab, M. Mozaffari, G.R. Amiri, J. Amighian, Preparation of cobalt–zinc ferrite ($\text{Co}_{0.8}\text{Zn}_{0.2}\text{Fe}_2\text{O}_4$) nanopowder via combustion method and investigation of its magnetic properties, *Materials Research Bulletin* 45 (2010) 1792–1795.
- [15] Z.G. Jia, D.P. Ren, Q.Z. Wang, L.X. Xu, Rongsun Zhu, Structural and magnetic properties of $\text{Co}_{1-x}\text{Zn}_x\text{Fe}_2\text{O}_4$ nanorods prepared by the solvothermal annealing method, *Ceramics International* 39 (2013) 6113–6118.
- [16] J. Ma, J.T. Zhao, W.L. Li, S.P. Zhang, Z.R. Tian, S. Basov, Preparation of cobalt ferrite nanoparticles via a novel solvothermal approach using divalent iron salt as precursors, *Materials Research Bulletin* 48 (2013) 214–217.
- [17] Y. Zhang, D.J. Wen, Effect of RE/Ni (RE=Sm, Gd and Eu) addition on the infrared emission properties of Co–Zn ferrites with high emissivity, *Materials Science and Engineering B* 172 (2010) 331–335.
- [18] E.W. Shi, C.T. Xia, W.Z. Zhong, B.G. Wang, C.D. Feng, Crystallographic properties of hydrothermal barium titanate crystallite, *Journal of the American Ceramic Society* 80 (1997) 1567–1572.
- [19] H.M. Zaki, S.F. Mansour, X-ray and IR analysis of Cu–Si ferrite, *Journal of Physics and Chemistry of Solids* 67 (2006) 1643–1648.
- [20] G.N. Kustova, E.B. Burgina, G.G. Volkova, T.M. Yurieva, L.M. Plyasova, IR spectroscopic investigation of cation distribution in Zn–Co oxide catalysts with spinel type structure, *Journal of Molecular Catalysis A—Chemical* 158 (2000) 293–296.
- [21] J.A. Duffy, Optical Absorption of $\text{Na}_2\text{O}-\text{WO}_3$ glass containing transition-metal ions, *Journal of the American Ceramic Society* 60 (1977) 440–443.
- [22] D.B. Zhu, J.S. Liang, Y. Ding, G. Xue, L.H. Li, Effect of heat treatment on far infrared emission properties of tourmaline powders modified with a rare earth, *Journal of the American Ceramic Society* 91 (2008) 2588–2592.
- [23] R.H. Pratt, Tutorial on fundamentals of radiation physics: interactions of photons with matter, *Radiation Physics and Chemistry* 70 (2004) 595–603.
- [24] S.M. Wang, K.M. Liang, Crystallization behavior and infrared radiation property of nickel–magnesium cordierite based glass–ceramic, *Journal of Non-Crystalline Solids* 354 (2008) 1522–1525.
- [25] N.S. Khot, B.P. Shinde, B.B. Ladgaonkar, S.C. Watawe Kale, Magnetic and structural properties of magnesium zinc ferrites synthesized at different temperature, *Advances Applied Sciences Research* 2 (2011) 460–471.
- [26] J.Z. Jiang, P. Wynn, S. Mørup, T. Okada, F. Berry, Magnetic structure evolution in mechanically milled nanostructured ZnFe_2O_4 particles, *Journal of Nanostructures Materials* 12 (1999) 737–740.
- [27] S.H. Sun, H. Zeng, D.B. Robinson, S. Raoux, P.M. Rice, S.X. Wang, G.X. Li, Monodisperse MFe_2O_4 (M=Fe, Co and Mn) nanoparticles, *Journal of the American Ceramic Society* 126 (2004) 273–279.